

See discussions, stats, and author profiles for this publication at: <https://www.researchgate.net/publication/223964318>

# Receptor-Mediated, Tumor-Targeted Gene Delivery Using Folate-Terminated Polyrotaxanes

ARTICLE in MOLECULAR PHARMACEUTICS · APRIL 2012

Impact Factor: 4.38 · DOI: 10.1021/mp200315c · Source: PubMed

CITATIONS

24

READS

35

9 AUTHORS, INCLUDING:



Yi Zhou

Guangzhou Medical University

3 PUBLICATIONS 39 CITATIONS

SEE PROFILE



Jian-Dong Luo

25 PUBLICATIONS 623 CITATIONS

SEE PROFILE



Jianhai Chen

9 PUBLICATIONS 63 CITATIONS

SEE PROFILE

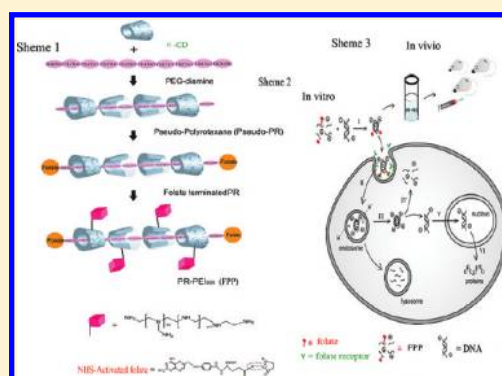
## Receptor-Mediated, Tumor-Targeted Gene Delivery Using Folate-Terminated Polyrotaxanes

Yi Zhou,<sup>†</sup> He Wang,<sup>‡</sup> Chengxi Wang,<sup>†</sup> Yueshan Li,<sup>§</sup> Wenfeng Lu,<sup>†</sup> Shuifang Chen,<sup>†</sup> Jiandong Luo,<sup>§</sup> Yongnan Jiang,<sup>†</sup> and Jianhai Chen<sup>\*,†</sup><sup>†</sup>Department of Pharmaceutical Science, Nanfang Hospital, Southern Medical University, Guangzhou 510515, China<sup>‡</sup>Institute for Cancer Research, Southern Medical University, Guangzhou 510515, China<sup>§</sup>Department of Pharmaceutical Science, Guangzhou Medical University, Guangzhou 510182, China

## S Supporting Information

**ABSTRACT:** Safe and effective gene delivery is essential to the success of gene therapy. We synthesized and characterized a novel nonviral gene delivery system in which folate (FA) molecules were functioned as blockers on cationic polyrotaxanes (PR) composed of poly(ethylenimine) (PEI)<sub>600</sub>-grafted  $\alpha$ -cyclodextrin rings linearized on polyethylene glycol to form FA-terminated PR-PEI<sub>600</sub> (FPP). The FA terminal caps of FPP target cell surfaces abundant in FA receptor (FR), a common feature of tumor cells. The structure of FPP was characterized by using <sup>1</sup>H nuclear magnetic resonance (<sup>1</sup>H NMR). The delivery particle was composed of chemically bonded PEG (4000),  $\alpha$ -cyclodextrins (CD), and PEI (600 Da) at a molar ratio of 1:17:86.7, and the particle size and zeta potential of FPP/pDNA polyplexes were measured using dynamic light scattering. FPP/pDNA exhibited a lower cytotoxicity, strong specificity to FR, and high efficiency of delivering DNA to target cells in vitro and in vivo with the reporter genes. Furthermore, the FPP/DNA complex showed an enhanced antitumor effect in the nude mice compared with other delivery systems, such as PEI-25K. Together, these results suggest that FPP may be useful for gene therapy.

**KEYWORDS:** poly(ethylenimine), supramolecule, cyclodextrin, folate receptor targeting, gene carrier



## ■ INTRODUCTION

Gene therapy shows great promise for the treatment of various human cancers and other diseases. It is known that gene delivery mainly depends on the carrier, which includes both virus- and nonvirus-based vector systems. Virus-based vectors, for example, the recombinant constructs from lentiviruses and adenoviruses, are a highly efficient means of gene transfection by delivery of exogenous DNA into host cells. However, safety issues raised by the toxicity, oncogenicity, and immunogenicity of viral vectors greatly hamper their routine use in both basic research and in the clinical setting. These safety concerns have provided an incentive to develop nonviral delivery systems particularly for the treatment of diseases where viral vectors have failed.<sup>1–3</sup> Although they have a lower gene transfer efficiency, nonviral vectors are easier to produce and modify, resulting in increased transfection efficiency and tissue specificity compared to viral vectors.

Cationic polymers are the most commonly used vector for nonviral gene delivery. They have been extensively investigated due to the ease with which their synthesis can be controlled, the presence of multivalent-functionalized surface amino groups, and their ability to compact nucleic acid.<sup>4–7</sup> For example, cationic poly-L-lysine, poly(ethylenimine) (PEI), poly-

(ethylene glycol) (PEG), dextrin, gelatin, and dendrimers have proved capable of transfecting genes to different cell lines.<sup>8,9</sup>

PEI is one of the best known and most widely studied cationic polymer-type nonviral gene delivery vectors.<sup>10</sup> Usually, high molecular weight PEI has a high gene transfection efficiency but potent cytotoxicity, whereas low molecular weight PEI (<2000 Da) has a weak gene transfection efficiency but lower cytotoxicity.<sup>11</sup> To achieve efficient gene transfection with low cytotoxicity, the conjugation of PEI with biodegradable materials such as cyclodextrins (CDs), chitosan (CHI), and poly(ethylene glycol) (PEG) has been suggested.<sup>12</sup>

Cyclodextrins (CDs) are macrocyclic oligosaccharides composed of 6, 7, or 8 D(t)-glucose units connected by  $\alpha$ -1,4-linkages and designated  $\alpha$ -,  $\beta$ -, or  $\gamma$ -CDs, respectively. The oligosaccharides have low immunogenicity and cytotoxicity in animals and humans<sup>13</sup> and can enhance the absorption and resistance to nucleases of oligonucleotides through complex formation.<sup>14</sup> CDs have been incorporated into cationic polymers to produce new gene delivery vectors.<sup>13</sup> For example,

**Received:** June 22, 2011

**Revised:** April 2, 2012

**Accepted:** April 7, 2012

**Published:** April 7, 2012

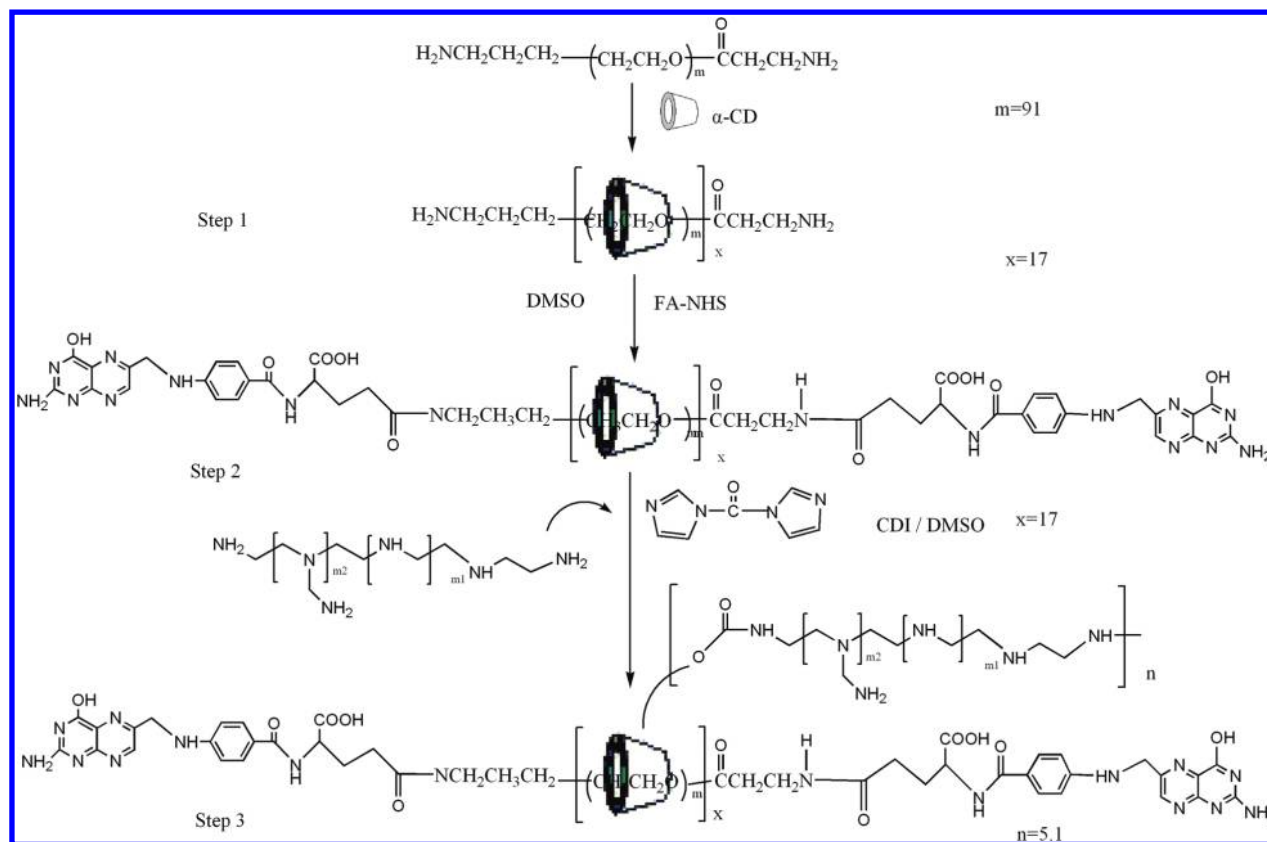


**Figure 1.** Proposed reaction scheme for FPP synthesis.

a class of linear and CD-based cationic polymers has been reported by Davis et al. for the efficient delivery of nucleic acids.<sup>6</sup> Li et al. subsequently demonstrated the utility of such polymers in gene delivery by threading cationically rendered  $\alpha$ -CD molecules through a PEG chain capped with bulky end-caps.<sup>15</sup> The star-shaped polymers and the cationic supramolecules showed excellent transfection efficiency in Cos7 and HEK293 cells.<sup>15,16</sup>

The backbone of polymeric gene carriers can be modified and optimized in a number of ways to achieve high efficiency of gene transfection. One such method is to introduce folate (FA)<sup>9</sup> to target folate receptors (FRs) which are overexpressed in certain cancer cells.<sup>17</sup> FA is particularly good for this application since it has low immunogenicity, low toxicity, and high affinity for FRs. We previously used FA to cap cationic polyrotaxanes (PRs) composed of camptothecin (CPT)-conjugated  $\alpha$ -CDs threaded on PEG (PR-CPT).<sup>18</sup> PR-CPT is biodegradable and displays a high water-solubility, antitumor effects, and low cytotoxicity in vitro and in vivo.

In the present study, we synthesized and characterized a cationic PR consisting of PEI<sub>600</sub>-grafted  $\alpha$ -CDs threaded on a homobifunctional PEG chain (PEI<sub>600</sub>-PR) with FA caps at both ends (FPP). The aim was to test the utility of FR-targeted cationic supramolecules as gene delivery systems in human oral squamous carcinoma cells (KB, cells overexpressing FRs) and human lung carcinoma cells (A549, cells with no FRs) in vitro or in vivo. We also evaluated the potential of the new vector in cancer gene therapy by binding the tumor suppressor gene p53 in vivo. Our results demonstrate that FPP can effectively condense plasmid DNA (pDNA) into small nanoparticles and improve gene-transfection efficiency in cells overexpressing FRs

compared with FR-negative cells and significantly improve antitumor effects in the cancer bearing nude mice.

## MATERIALS AND METHODS

**Reagents.** PEI (600 and 25000 Da, branched chain),  $\alpha$ -cyclodextrin (985 Da), FA (441.4 Da), triethylamine (Et<sub>3</sub>N), dimethyl sulfoxide (DMSO), 1,1'-carbonyldiimidazole (CDI), and Boc-L-tyrosine hydroxysuccinimide ester (BOC-Tyr-OSu) were obtained from Sigma-Aldrich (St. Louis, MO, USA). PEG-bilateral amino (PEG-BA; -NH<sub>2</sub>-PEG-NH<sub>2</sub>, 4000 Da) was purchased from Beijing Kaizheng Biotech (China). D-Luciferin potassium salt (*syn*) was obtained from Caliper Life Sciences (Hopkinton, MA, USA).

**Synthesis and Characterization of FPP Polymer.** The active ester of FA was prepared as described previously.<sup>19</sup> Briefly, FA (0.30 g, 0.68 mmol) and triethylamine (0.15 mL, 1.0 mmol) were dissolved in dry dimethyl sulfoxide (DMSO) (10 mL) and combined with dicyclohexylcarbodiimide (0.14 g, 0.68 mmol). The solution was stirred for 1 h at room temperature in the dark, and *N*-hydroxysuccinimide (NHS; 0.12 g, 1.0 mmol) was added. The mixture was stirred overnight in the dark at room temperature, filtered through glass wool to remove dicyclohexylurea, and precipitated with diethyl ether. The active ester of FA was collected by filtration, washed with dry tetrahydrofuran (THF), and vacuum-dried. The synthesis of PEI-polyrotaxanes (PEI-PR) is depicted in Figure 1. A pseudo-PR consisting of  $\alpha$ -CDs and PEG-BA 4000 was prepared as previously reported.<sup>16</sup> PEG-BA 4000 (1 g,  $5 \times 10^{-4}$  mol) dissolved in 5 mL of water was added to a saturated aqueous solution of  $\alpha$ -CD (11 g,  $1.2 \times 10^{-2}$  moles) at room temperature and ultrasonically agitated for 1 h, followed by stirring for 24 h. Precipitated pseudo-PR was collected by centrifugation, washed

three times with distilled water, dried under vacuum, and stored at room temperature (Figure 1, Step 1). To cap the terminal amino groups of the pseudo-PR with FA, FA-NHS (5.0 g) and the pseudo-PR (11.67 g) were dissolved in dry DMSO (50 mL) and stirred for 96 h at room temperature. The FA-terminated PR polymer was precipitated with acetone, collected by centrifugation, washed with ethanol and water, and dried at room temperature (Figure 1, Step 2). The Boc-Tyr-terminated PR polymer was synthesized as described previously.<sup>20</sup> PEI<sub>600</sub>-PR conjugates were synthesized as previously described<sup>21</sup> (Figure 1, Step 3). FA and Boc-Tyr-terminated PR polymers (0.31 g, 0.011 mmol) were dissolved in 20 mL of dry DMSO under nitrogen, and the solution was added dropwise for 6 h under nitrogen to 20 mL of anhydrous DMSO containing dissolved CDI (2.56 g, 15.75 mmol). The mixture was stirred overnight under nitrogen at room temperature and then combined with 100 mL of THF and 200 mL of diethyl ether to precipitate the product. The precipitate was centrifuged, washed three times with THF, dissolved in 10 mL of DMSO, and added dropwise with stirring at room temperature for 3 h to 5.49 mL (18.9 mmol) of PEI<sub>600</sub> dissolved in 10 mL of DMSO. Stirring was continued overnight, 250 mL of THF was added, and the precipitate centrifuged and washed three times with THF. The resulting crude product was dialyzed (MW cutoff 8000) and eluted with deionized water. Yields of 0.12 g (30%) and 0.14 g (31%) of brown solids were obtained, deemed to be FA-terminated PR-PEI<sub>600</sub> (FPP) and Boc-Tyr-terminated PR-PEI<sub>600</sub> (BPP), respectively.

**Characterization of Polymers.** The composition of FPP was estimated by <sup>1</sup>H nuclear magnetic resonance (<sup>1</sup>H NMR) spectroscopy measured on an AVANCE 600 FT-NMR (Bruker, Germany). Prior to analysis, samples were dissolved in deuterated water (D<sub>2</sub>O) or DMSO depending on solubility at room temperature.

**Preparation of Plasmids.** A reporter plasmid expressing enhanced green fluorescent protein (from pAAV-EGFP) and luciferase (from pGL3-luc) designated pEGFP-luc was cloned. The expression of plasmid PcDNA3.1-p53 was constructed by inserting the enhancing green fluorescent protein (EGFP) and p53 gene into pcDNA3.1(-B). Plasmid DNAs were amplified in *Escherichia coli* and purified according to the supplier's protocol (Qiagen, Hilden, Germany). The purity and concentration of the purified pDNA were determined by absorption at 260 and 280 nm and by agarose gel electrophoresis. The purified plasmid DNA was maintained in aliquots at a concentration of 1 µg/mL.

**Preparation and Characterization of FPP/pDNA Complexes.** FPP/pDNA complexes were prepared just before use in 150 mmol/L NaCl by combining equal volumes of polymer solutions, gently vortexing, incubating at room temperature for 30 min, and filtering through a 0.45 mm syringe. Hydrodynamic particle size and zeta potential of the polyplexes were measured at 37 °C by dynamic light scattering using a Zetasizer 3000 (Malvern Instruments, Worcestershire, UK). Polyplexes with different lipid nitrogen/DNA phosphate (N/P) ratios had a final pDNA concentration of 10 µg/mL. Measurements were performed in triplicate to obtain z-average diameters (nm) and mean zeta potentials (mV).

**Gel Retardation Assay.** To confirm the ability of the polymers to condense pDNA, electrophoresis was performed. Complex formation was induced at N/P = 1–10 in a final volume of 6× agarose gel loading dye (10 µL total). Each mixture was vortexed, incubated for 30 min at room

temperature, and analyzed on 1% agarose gel in TAE running buffer (40 mM Tris-acetate, 1 mM EDTA) for 40 min at 80 V using a Sub-Cell system (Bio-Rad, Hercules, CA, USA). The gel was stained with ethidium bromide (0.5 µg/mL), and DNA bands were visualized and photographed under a UV transilluminator with a BioDoc-It imaging system (UVP, Upland, CA, USA).

**Cell Lines, Cell Culture, and Cell Viability Assays.** The following human cell lines were cultured in Dulbecco's modified Eagle medium (DMEM, Gibco BRL, Paris, France): embryonic kidney cells (HEK 293T, FR positive cells),<sup>22</sup> oral squamous carcinoma cells (KB, FR positive cells), cervical carcinoma cells (HeLa, FR positive cells), colon cancer cells (LoVo), lung carcinoma cells (A549, FR negative cells), and bronchial epithelial cells (16HBE). All media were supplemented with 10% fetal bovine serum (FBS; HyClone, Logan, UT), 100 µg/mL streptomycin, and 100 U/mL penicillin. Cells were seeded at  $1 \times 10^4$ /well in 96-well plates and incubated at 37 °C in a humidified, 5% CO<sub>2</sub> atmosphere for 18–24 h to reach 80% confluence. Cells were washed with PBS prior to 4 h exposure to polymer/DNA complexes. Fresh, serum-free media containing various amounts of polymers or polymer/pDNA complexes at various N/P ratios (5, 10, 15, 20, 30, and 40) and concentrations (5, 50, 100, 200, 300, and 500 µg/mL) were applied. After 24 h, media were replaced with growth media containing 20 µL of Cell Titer 96 AQueous One Solution (Promega, Madison, WI). Following 3 h of incubation, the absorbance was measured at 570 nm using a GLR 1000 ELISA plate reader (Genelabs Diagnostics, Singapore) to obtain the metabolic activity of the cells.

**Gene Transfection in Vitro.** Cells were seeded in 24-well plates at an initial density of  $1 \times 10^5$ /well in 1 mL aliquots of growth medium. After incubation for 18 h to 80% confluence, media were replaced with polymer/pGL3-control polyplexes (1 µg) at various N/P ratios and 400 µL of Opti-MEM (Invitrogen, Carlsbad, CA) in each well. After incubation for 4 h at 37 °C, the media was replaced with fresh growth media and cells maintained for 24 or 48 h. To determine the effect of FBS on transfection efficiency, Opti-MEM containing various concentrations of FBS was used as the transfection medium. To visualize the expression of EGFP and luciferase in cancer cells transfected with FPP/pEGFP-luc, a microscopic evaluation of EGFP expression and the luciferase assay were performed 48 h post-transfection. Luciferase expression was assayed according to the manufacturer's protocol (TB281, Promega). Microscopic evaluation of EGFP expression in different cell lines was performed as described previously.<sup>23</sup> The transfection efficiency was evaluated by scoring the percentage of cells expressing EGFP using a FACSCalibur System (Becton-Dickinson, San Jose, CA). Fluorescence parameters from 10 000 cells were acquired, and transfections were performed in triplicate. The transfection efficiency was expressed in relative light units.

**In Vivo Study. Establishment of the KB Melanoma-Bearing Nude Mice Model.** Nude mice (4–6 weeks, 18–22 g weight) were purchased from the Laboratory Animal Center, Southern Medical University (Guangzhou, China) and maintained in a pathogen-free environment with controlled temperature (24 °C). Animal experiments were conducted in accordance with national regulations and the approval of the University of Guangdong Animal Care and Use Committee. KB cells ( $1 \times 10^7$  cells/mL) were injected subcutaneously (0.1 mL;  $1 \times 10^6$  cells) into the right dorsal flank of nude mice. When the melanoma size reached 4 mm in diameter (within 14 days),



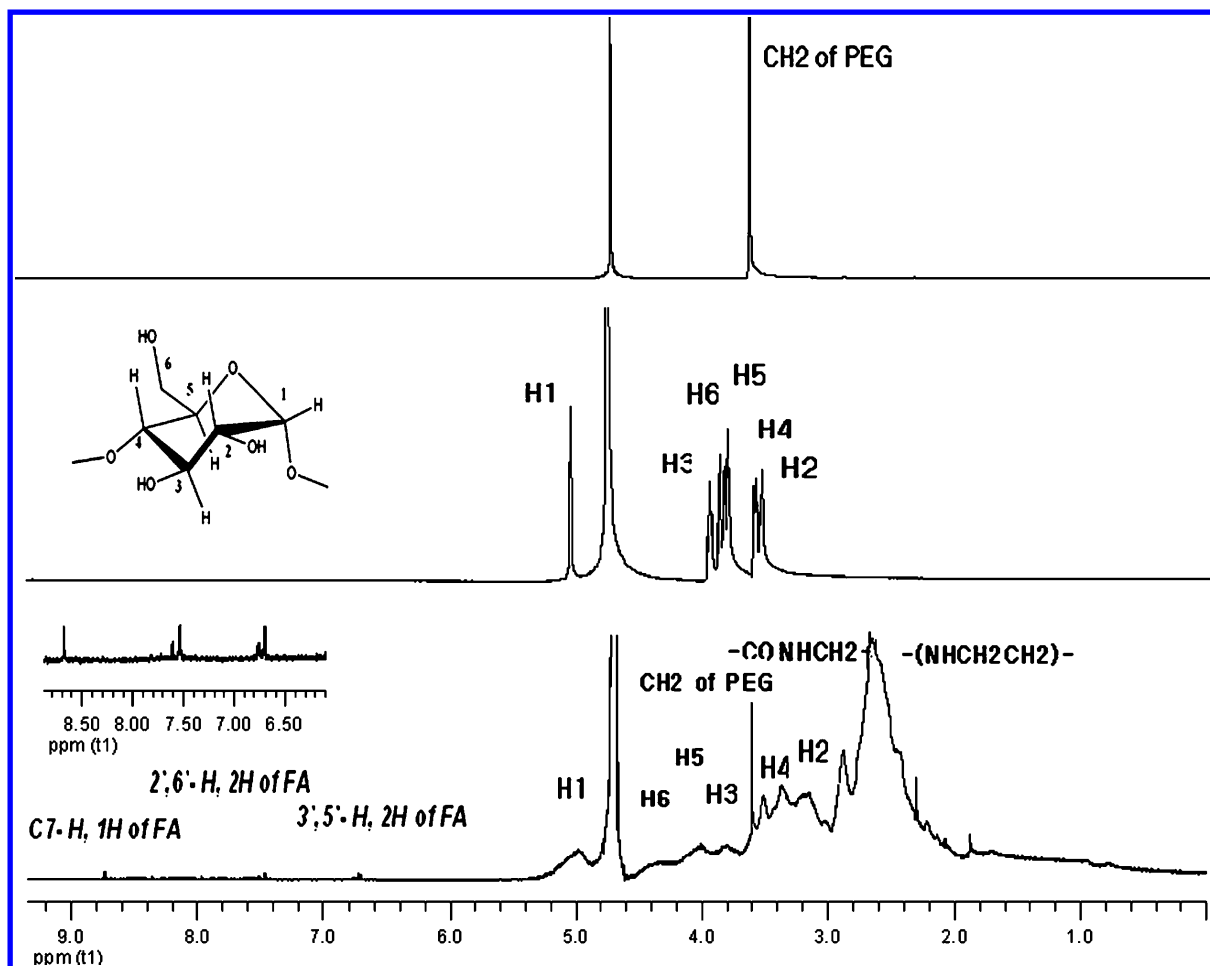


**Figure 2.** Representative  $^1\text{H}$  NMR spectrum of FPP in  $\text{D}_2\text{O}$ :  $\delta = 3.5\text{--}3.6$  ppm ( $-\text{CH}_2\text{CH}_2\text{O}-$ , PEG ethylene),  $4.0\text{--}3.0$  ppm ( $\text{H}_3$ ,  $\text{H}_6$ ,  $\text{H}_5$ ,  $\text{H}_4$ ,  $\text{H}_2$  of  $\alpha\text{-CD}$ ),  $6.7$  ppm (d,  $3'$ ,  $5'$ -H,  $2\text{H}$ ),  $7.5$  ppm (d,  $2'$ ,  $6'$ -H,  $2\text{H}$ ), and  $8.7$  ppm (s,  $\text{C}_7\text{-H}$ ,  $1\text{H}$ ) for FA.  $3.0\text{--}2.0$  ppm ( $-\text{CONHCH}_2-$ ,  $-\text{NHCH}_2\text{CH}_2-$  of PEI).

the mice were randomly assigned to five groups ( $n = 15$  per group) and injected intratumorally or via the tail vein with the following polyplexes: FPP/pEGFP-luc ( $50\text{ }\mu\text{g}$  plasmid DNA) and BPP/pEGFP-luc ( $N/P = 20:1$ ), naked pEGFP-luc ( $50\text{ }\mu\text{g}$  of plasmid DNA), or PEI-25 kDa/pEGFP-luc ( $N/P$  ratio =  $10:1$ ), lipofectamine/pEGFP-luc ( $50\text{ }\mu\text{g}$  of plasmid DNA).<sup>24</sup>

**Luciferase Assay of Tumor Tissue Homogenates.** Nude mice with tumors were sacrificed 24 and 48 h after injection. All tumor nodules were then extracted and weighed. Tumor tissue was collected and homogenized in cell lysis buffer. Tissue lysates were then centrifuged at  $14\,000\text{ g}$  for  $5\text{ min}$  at  $4\text{ }^\circ\text{C}$  and  $30\text{ }\mu\text{L}$  of supernatant used to determine luciferase activities using the luciferase assay in accordance with the manufacturer's protocol (TB281, Promega).

**Antitumor Activity in Vivo after p53 Gene Transfection.** Nude mice bearing tumors with a diameter  $4\text{--}6\text{ mm}$  (reached within 14 days) were inoculated with  $1 \times 10^6$  KB cells and randomly assigned to five groups ( $n = 15$  per group). They were then injected into the tail vein with a mixture of  $50\text{ }\mu\text{g}$  of p53 plasmid (pcDNA3.1-p53) and polymers in a total volume of  $0.1\text{ mL}$  of PBS. The treatment was conducted four times at 6 day intervals. The control group received equal volumes of PBS according to the same protocol. Tumor weight was recorded every 5 days until the 25th day when all mice were sacrificed and the tumors dislodged, weighed, and examined by Western blot analysis.

**Western Blot Analysis of p53 and Bax in Tumor Tissue.** Electrophoresis and immunoblotting were performed as previously described.<sup>25</sup> The blotted membranes were probed with the respective primary polyclonal antitumor antibodies for caspase-9 and bax (all from Peprotech) or  $\beta$ -actin (as loading control; Sigma-Aldrich, China) overnight at  $4\text{ }^\circ\text{C}$ . They were then incubated with the respective IgG HRP secondary antibodies (Santa Cruz) for  $1\text{ h}$  at room temperature. Upon incubation in the ECL Western blotting detection reagent (Amersham), the protein bands were visualized by autoradiography on X-ray film (Fuji, Japan). Densitometric analysis was done by Quantity One version 4.4.1 Basic (BioRad), and the relative density of the protein bands was calculated after being normalized with  $\beta$ -actin.

**Hematoxylin and Eosin (HE) Staining of Liver and Spleen.** Tumor-bearing mice were administered a tail vein injection of FPP/DNA ( $50\text{ }\mu\text{g}$  of DNA,  $N/P = 20, 40, 60$ ) or an equal volume of naked DNA (as a control) and then treated as described above. After 25 days, the extracted tumors were fixed with 4% formaldehyde and embedded in paraffin. Sections  $5\text{ }\mu\text{m}$  thick were cut, deparaffinized, rehydrated, and then stained with HE prior to further histological analysis under a light microscope.

**Statistics Analyses.** Results are expressed as means  $\pm$  standard deviation (SD) of triplicate determinations (or as representative data from one or two independent experiments).

Data were submitted to normality and equal variance tests which revealed normal distributions. ANOVA and a multiple comparisons test were made in statistical analysis using SPSS 13.0. Differences were considered statistically significant at  $p < 0.05$ .

## RESULTS

**Synthesis and Characterization of FPP.** FA was used to cap the primary amino groups of the pseudo-PR backbone through a CDI-coupling reaction involving the terminal carboxylate group of FA (Supporting Information, Figure S1). The composition of FA-terminated PR-PEI<sub>600</sub> was confirmed by <sup>1</sup>H NMR (Figure 2). Signals corresponding to PEG were observed at 3.7 ppm ( $-\text{[CH}_2\text{CH}_2\text{O]}_n-$ ). The C1 and C2–C6 protons of  $\alpha$ -CD were identified at 4.9 ppm and 3.0–4.2 ppm, respectively. Signals arising from FA in polymers were in the range 6.5–8.7 ppm and signals of PEI ethylene protons ( $-\text{CH}_2\text{CH}_2\text{NH}-$ ) in FPP were observed at 2.4–3.0 ppm. The determination of the ratio of PEG,  $\alpha$ -CD, and PEI peak areas in FPP showed FPP was composed of chemically bonded PEG,  $\alpha$ -CD, and PEI (600 Da) in the molar ratio 1:17:86.7. Thus the grafting rate for  $\alpha$ -CD is 85%. These results are consistent with the expected chemical structures of the polymers. However, it is difficult to calculate the molecular weight of the gene vector since there was partial cross-linking between PEI and PR.

**Complex Formation of FPP and Plasmid DNA.** The ability of FPP to condense pDNA into particulate structures was demonstrated by agarose gel electrophoresis and the determination of particle size and zeta potential. As shown in Figure 3, FPP compacted pDNA entirely at  $N/P = 2$ –3 using gel retardation by comparing cationic polymers/pDNA complexes with increasing  $N/P$  ratios to branched PEI-25 kDa/pDNA complexes. This indicates that the polymers have a slightly lower DNA condensation capacity than PEI-25 kDa. The particle size of FPP/pDNA complexes decreased sharply with increasing  $N/P$  ratios and no complex was larger than 140 nm in diameter at  $N/P = 20$ . Complexes stabilized to a range of 75–200 nm for  $N/P > 4$  (Figure 4a). These results are similar to those observed in branched PEI-25 kDa/pDNA complexes. In contrast, the zeta potential of the complexes increased as  $N/P$  increased from 2 to 6 and stabilized at  $N/P \geq 10$ . At  $N/P > 10$ , the zeta potential of the complexes of pDNA PEI (25 K) was strongly positive and varied in the same range (20–30 mV) which results in a similar affinity for the cell surface regardless of FR overexpression<sup>26</sup> (Figure 4b).

**Cytotoxicity of Polyplex.** The cytotoxicity of FPP to HeLa and 16HBE cells was assessed at various FPP concentrations using cells incubated with culture media as controls (Figure 5a). The cell viability decreased dramatically with the increase in PEI-25 kDa concentration, whereas FPP and BPP were not cytotoxic to either cell line (Figure 5a,b). Cell viabilities in response to FPP/pDNA and BPP/pDNA complexes were also assayed at various  $N/P$  ratios (Figure 5c,d). The cell viability was significantly higher on exposure to FPP/pDNA and BPP/pDNA complexes than to PEI-25 kDa/pDNA complexes for  $N/P < 20$ . Even for  $N/P > 40$ , FPP maintained higher cell survival. No significant difference in cytotoxicity of FPP and BPP to HeLa cells was observed at the same  $N/P$  ratios and concentration. These results are consistent with the half maximal inhibitory concentration ( $\text{IC}_{50}$ ) values of FPP in HeLa and 16HBE cells of 162 and 178  $\mu\text{g/mL}$ , respectively.

**Transfection Efficiency in Vitro.** Because of their high cell-surface expression of FRs, KB cells are commonly used to

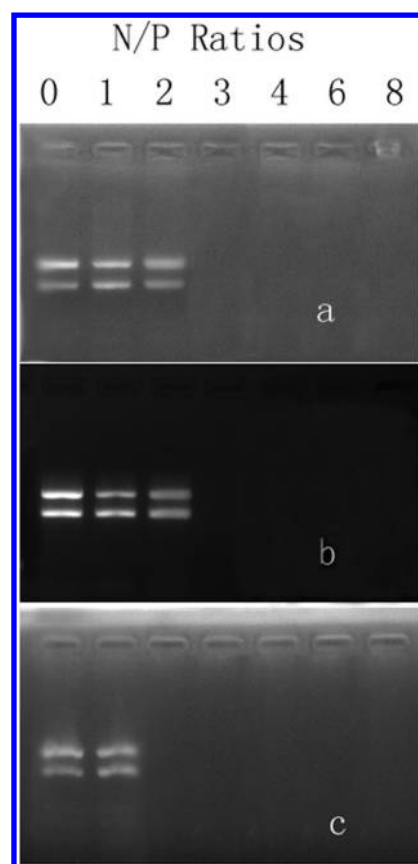


**Figure 3.** Electrophoretic mobility of plasmid DNA in (a) FPP/pDNA, (b) BPP/pDNA, and (c) PEI-25 kDa/pDNA complexes at various  $N/P$  ratios.

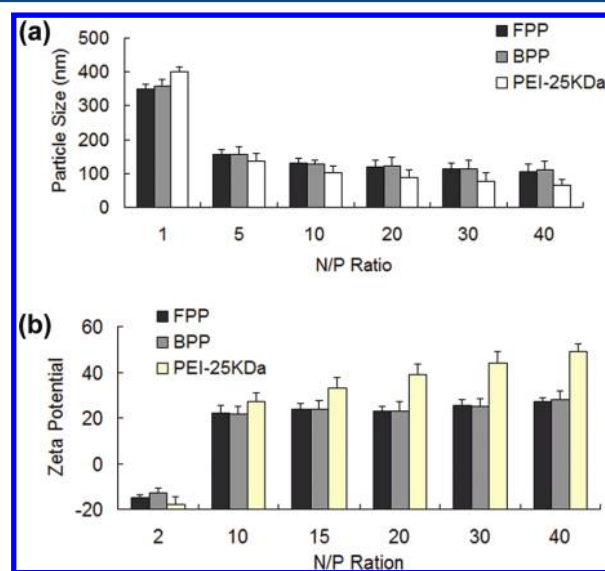


**Figure 4.** (a) Particle sizes and (b) zeta potential of FPP/pDNA, BPP/pDNA, and PEI-25KDa/pDNA at various  $N/P$  ratios.

study functional biopolymers with appended FA groups. To determine the optimal  $N/P$  ratio of FPP/pDNA complexes for transfection, KB cells were transfected with FPP/pEGFP-luc complexes with  $N/P$  ratios of 10, 15, 20, and 30 (Figure 6a). Luciferase activity in FPP/pEGFP-luc-transfected cells was higher than in BPP/pEGFP-luc-transfected cells by factors of 5, 13, 23, and 20, respectively ( $p < 0.01$ ,  $n = 4$ , Student's  $t$ -test). In

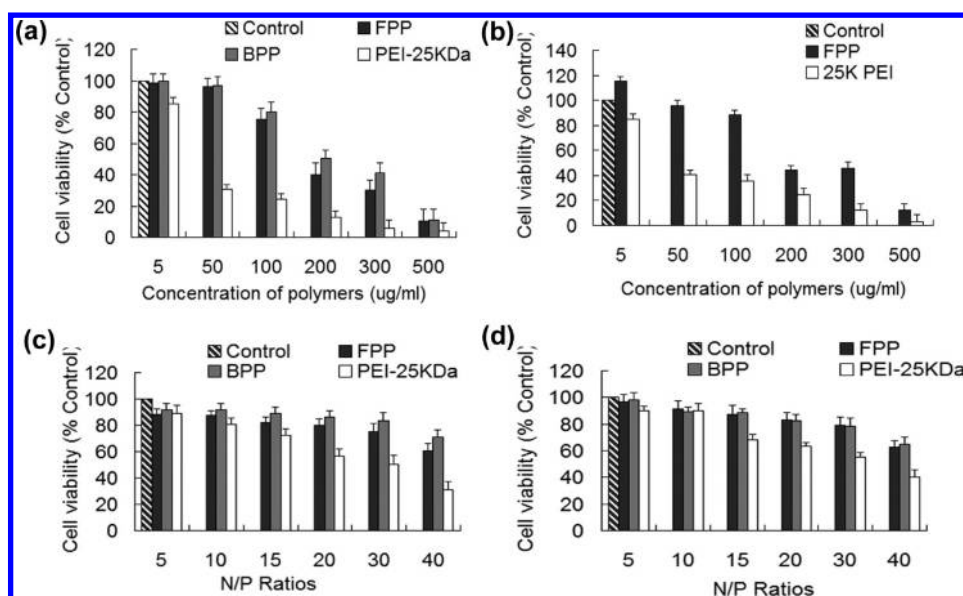


**Figure 5.** Polymer cytotoxicity at various concentrations to (a) HeLa and (b) 16HBE cell lines and cytotoxicity following transfection of the polymers/pDNA complexes in (c) HeLa and (d) 16HBE cell lines at various N/P ratios (data are means  $\pm$  SD,  $n = 4$ ).

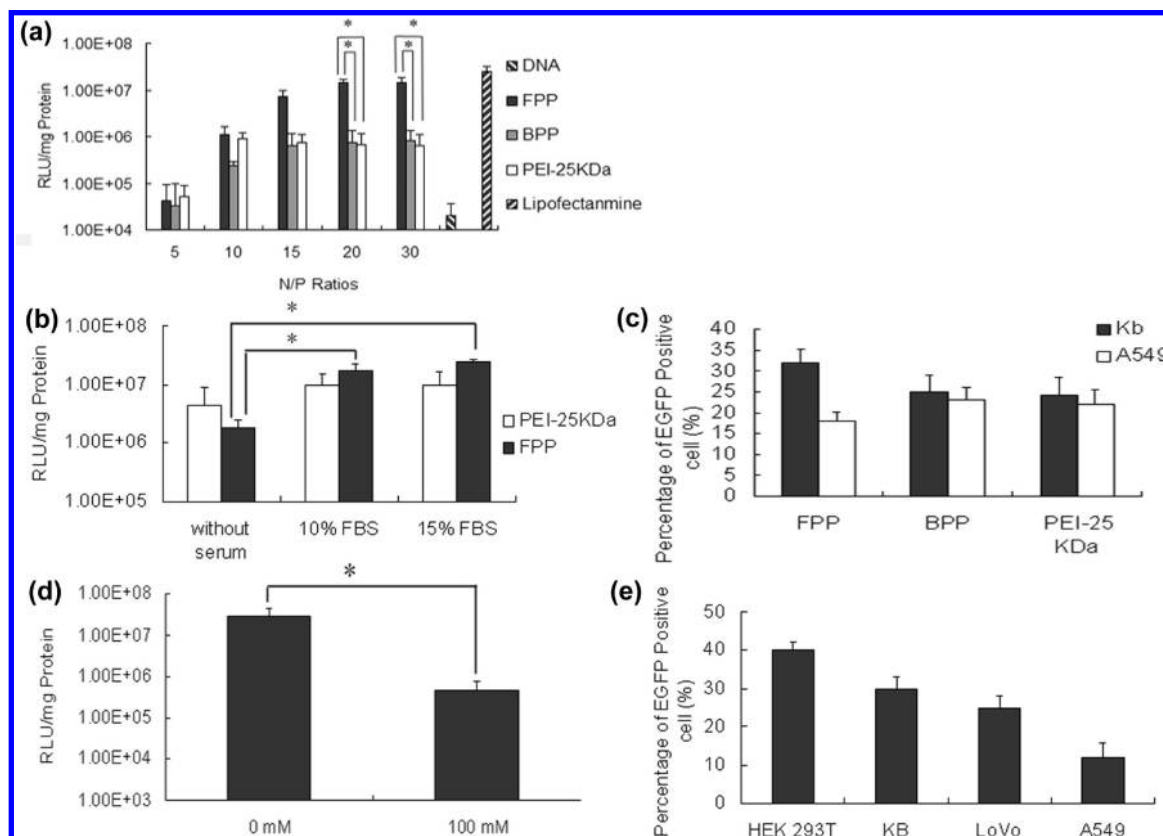


**Figure 6.** FPP-mediated luciferase and EGFP expression in vitro. (a) Optimal N/P ratios determined using the luciferase assay for FPP/pEGFP-luc, BPP/pEGFP-luc, and PEI-25KDa/pEGFP-luc (10% FBS) in KB cells. At N/P = 20, a significant difference was observed between FPP/pEGFP-luc and BPP/pEGFP-luc ( $p < 0.01$ ,  $n = 4$ , Student's  $t$ -test). (b) The effects of FBS in the transfection media were confirmed by luciferase expression assays for FPP/pEGFP-luc (1  $\mu$ g DNA, N/P = 20) and PEI-25 kDa/pEGFP-luc (1  $\mu$ g of DNA, N/P = 10). Significant differences in luciferase expression between serum-free and FBS preparations were detected by two polymer types ( $p < 0.01$ ,  $n = 4$ , Student's  $t$ -test). (c) Summary of percent EGFP expression in HeLa and A549 cells. (d) Competition assay of FPP/DNA complexes prepared at a charge ratio of 20 performed in the presence of FA (100 mM) to compete with the FA functional group of FPP for FR sites ( $p < 0.01$ ,  $n = 4$ , Student's  $t$ -test). (e) A panel of four different cell types evaluated for EGFP expression 48 h after transfection with FPP/pEGFP-luc polyplexes.

the absence of serum, FPP/pDNA at N/P = 20 showed a much lower transfection efficiency than PEI-25 kDa/pDNA at N/P =

10 in KB cells. The luciferase activities in FPP/pEGFP-luc-transfected cells were 8.7-fold and 11.4-fold higher in the



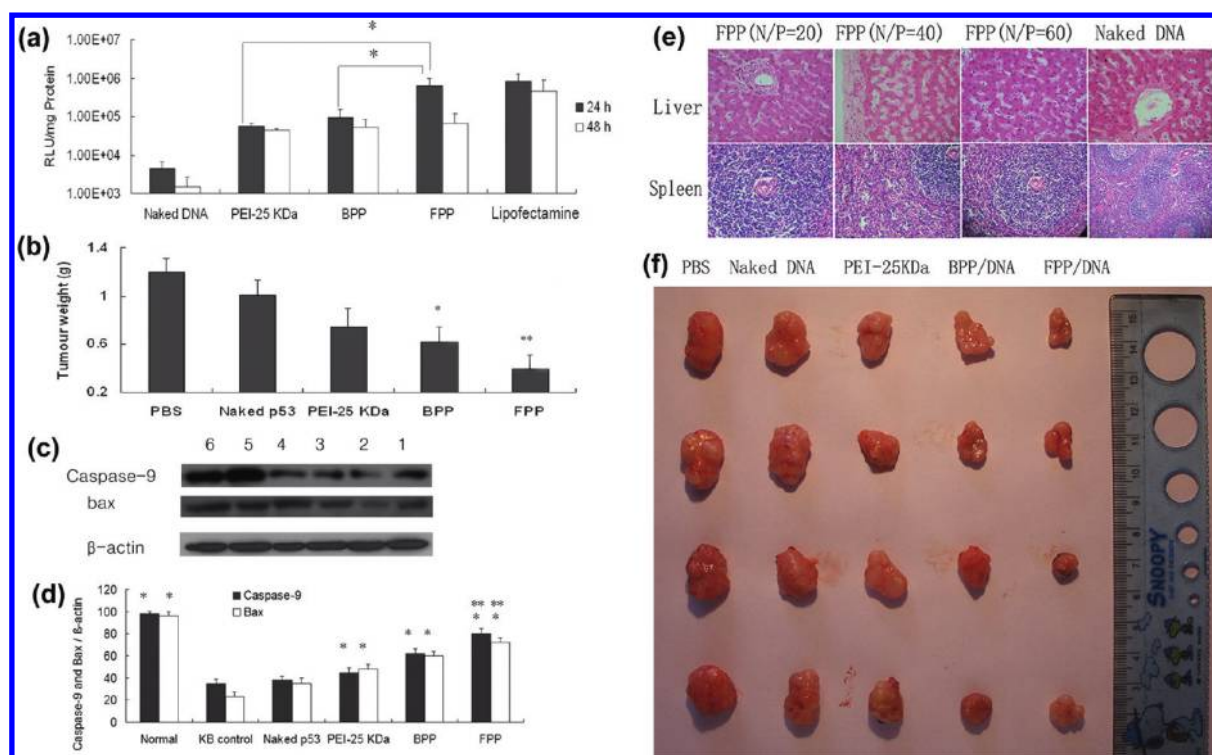


**Figure 7.** Transfection efficiency and toxicity of FPP in vivo. (a) Luciferase unit (RLU) of tumor tissue homogenates at 24 h after intratumoral injection. The level of luciferase expression induced by FPP/pEGFP-luc transfection was significantly higher than those mediated by PEI-25 KDa/pEGFP-luc and BPP/pEGFP-luc transduction ( $p < 0.01$ ,  $n = 4$ ). (b) Tumor growth inhibition in mice after receiving PBS, naked DNA (p53) plasmid, PEI-25 KDa/DNA (p53), BPP/DNA (p53), and FPP/DNA (p53) complexes. The weights of dislodged tumors from the mice treated with FPP/DNA (p53) were the minimum and about one-sixth of the tumor weights in the PBS group and clearly lower than that in BPP ( $p < 0.01$ ,  $p < 0.05$ , respectively,  $n = 4$ ). (c) Expression of caspase-9 and bax in mice treated with various complexes. (d) Expression of caspase-9 and bax in mice treated with FPP/DNA (p53) is significantly higher compared with those in the KB control group. Moreover, there is a clear difference between the BPP and FPP groups ( $p < 0.01$  and  $p < 0.05$ , respectively,  $n = 4$ ). Lane 1: normal control, Lane 2: KB control, Lane 3: naked p53, Lane 4: PEI-25KDa, Lane 5: BPP, Lane 6: FPP. (e) Images of dislodged tumors and HE staining did not detect any toxic response in liver and spleen (f) in tumor-bearing mice 25 days after tail vein injection of the various complexes.

presence of 10% FBS and 15% FBS, respectively, than in the absence of FBS (Figure 6b;  $p < 0.01$ ,  $n = 4$ , Student's *t*-test). Similarly, the luciferase activities in PEI-25 kDa/pEGFP-luc transfected cells were 2.6-fold and 3.1-fold higher in the presence of 10% FBS and 15% FBS, respectively, than in the absence of serum.

The transfection ability of FPP/pDNA was superior to that of BPP/pDNA and PEI-25 kDa/pDNA in KB cells. However, this difference in transfection capacity was not observed in terms of EGFP expression in transfected A549 cells (Figure 6c) indicating that the FA ligand on FPP plays a significant role in FR recognition and enhanced transfection efficiency in KB cells. Interestingly, the transfection efficiency of FPP/DNA complexes was clearly decreased in the presence of excess free FA (100 mM), suggesting that FPP/DNA complexes were absorbed via receptor-mediated endocytosis (Figure 6d). The gene transfection efficiency of FPP/pDNA in various tumor cell lines (293T, KB, LoVo, and A549) was evaluated according to the optimized transfection conditions ( $N/P = 20$ , 10% FBS). The transfection efficiency of FPP/pEGFP-luc polyplex assessed by EGFP expression was approximately 24–40% in 293T, KB, and LoVo cells (Figure 6e). In contrast, transfection efficiency in A549 cells which do not express FRs was only 18% (Supporting Information, Figure S2). Overall, FPP shows potent transfection efficiency and tissue specificity to FR positive cells.

**In Vivo Study. Luciferase Assay in Vivo.** Polymer/pEGFP-luc complexes containing 50  $\mu$ g of plasmid with  $N/P = 20$  were injected intratumorally into nude mice bearing KB tumors. The luciferase expression of tumor tissue was examined 24 and 48 h postinjection using a luminometer. At 24 h, FPP improved gene transfection efficiency by factors of 6.1 and 5.6 over PEI-25 KDa ( $N/P = 10$ ) and BPP, respectively. The luciferase activity of FPP/pEGFP-luc tumor cells increased by factors of 136 and 0.74 compared to those of naked/pEGFP-luc and lipofectamine/pEGFP-luc tumor cells, respectively (Figure 7a). Surprisingly, the luciferase activity in FPP/pEGFP-luc-injected tumors decreased 10-fold at 48 h, and the absorbed value in FPP is about 50% more than that in lipofectamine/pEGFP-luc-injected tumor.

**Antitumor Activity Assay.** The p53 tumor suppressor gene is widely applied in clinical treatment.<sup>27</sup> In the current study, FPP was used to delivery plasmid DNA pcDNA3.1-p53 into tumor cells. Tumor weights at 25 days in the FPP group were obviously decreased compared to those in the BPP/DNA (p53), PEI-25 kDa/DNA (p53), naked DNA (p53) (Figure 7e) and PBS control groups (Figure 7b) (all  $p < 0.01$ ). This clearly indicates that both FPP/DNA (p53) complexes are effective in inhibiting tumor growth.

Up-regulation of caspase and bax proteins was increased markedly by p53 gene treatment.<sup>28</sup> Thus, expression of caspase-9 and Bax was significantly increased in the PEI-25 KDa/DNA (p53), BPP/DNA (p53), and FPP/DNA (p53) groups



compared to the control group (all  $p < 0.01$ ). Up-regulation of apoptotic genes was also observed in the FPP group compared to the BPP group ( $p < 0.05$ ) (Figure 7c,d).

HE staining of liver and spleen from mice with KB tumors was performed 25 days after FPP/DNA (p53) (50  $\mu$ g of DNA, N/P 20:1, 40:1, and 60:1) tail vein injections. As shown in Figure 7f, the classic structure of a liver lobule with central vein is clearly seen after treatments. There was no evidence of hepatocellular degeneration or necrosis and no neutrophil, lymphocyte, or macrophage infiltration. The spleen sinus showed no pathological changes. Even at N/P = 60, nude mice could safely tolerate the FPPs/pLuc. These results are similar to those of in vitro cytotoxicity studies, showing that FPP at N/P = 40 did not show substantial cytotoxicity.

## DISCUSSION

Previously PRs have been shown to exhibit low toxicity and highly efficient gene transfection ability in vitro.<sup>29</sup> In the current study, FA was used to cap PR in the successful synthesis of FPP (Figure 2a,b). Furthermore, the results showed that FPP was composed of chemically bonded PEG,  $\alpha$ -CD, and PEI (600 Da) in a molar ratio of 1:17:86.7. Transfection of FPP in HEK 293, KB, LoVo, and A549 cell lines (Figure S2 of the Supporting Information) strongly demonstrated that grafting an appropriate amount of branch PEI chains to FA-terminated PR could remarkably improve the vector's ability to mediate gene delivery.

The toxicity of a gene delivery vector is the primary concern relating to its application in vivo because branch PEIs grafted in polymers induce high toxicity. Usually, the cytotoxicity of cationic polymers increases with increasing zeta potential. The zeta potential of the PEI-25 kDa/pDNA polyplexes with N/P > 10 was greater than 30 mV<sup>23</sup> whereas the zeta potential of FPP/pDNA polyplexes with N/P < 40 was less than 30 mV. This finding suggests that the lower cytotoxicity of FPP/pDNA polyplexes is due to their lower charge density (Figure 4b). In addition, FPP/pDNA polyplexes showed an optimum particle size for entry into tumor cells (Figure 4a). To evaluate the stability of the complexes, the ability of polymers with N/P = 0–8 to condense pDNA and affect gene transfection of complexes in media with or without serum was tested. The gel retardation results demonstrate that FPP with N/P = 2–3 completely compacts pDNA, indicating that these complexes have good stability. Importantly, the transfection efficiency of FPP/pDNA was enhanced in the presence of 10% or 15% FBS (Figure 6b) and was significantly higher than that of PEI-25K/pDNA in FBS.

It has been reported that the cytotoxicity of gene delivery carriers is due to the accumulation of nondegraded and nondischarged polymers with a large molecular weight and charge.<sup>30</sup> PEG, which is known to reduce the cytotoxicity of PEI amino groups,<sup>31</sup> resulted in lower cytotoxicities of FPP and BPP. The cytotoxicity of cationic polymers is most probably due to polymer aggregation on cell surfaces resulting in impaired membrane function. Cationic polymers also interfere with critical intracellular processes. For instance, the primary amine of PEI disrupts protein kinase C activity.<sup>26</sup> PEI, especially high molecular weight PEI, induces higher cytotoxicity than other biodegradable materials. Modified vectors in which the zeta potential is reduced can effectively decrease cytotoxicity.<sup>32</sup> We found that the cytotoxicities of FPP/pDNA and BPP/pDNA to HeLa cells were similar to their cytotoxicities to 293T, KB, LoVo, and A549 cells at

various N/P ratios. The lower cytotoxicity of FPP to 16HBE cells suggests that the polymer has a reduced effect in noncancerous tissue (Figure 5). However, compared with BPP, FPP induces lower viability in HeLa cells but not in 16HBE cells suggesting that the overexpression of FRs on the HeLa cell surface contributes to enhanced uptake of FPP via FR-mediated endocytosis.

The transfection efficiency and transgene expression level are the most important features of copolymers. We found that the transfection efficiency of FPP in KB cells, where the expression of FRs is high, was significantly enhanced compared to that of BPP (Figure 6a) in vitro. Consistently, the transfection efficiency of FPP was markedly attenuated in A549 cells in which FRs are not expressed. These results indicate that FR-mediated endocytosis may contribute to the high transfection efficiency of FPP. Furthermore, inhibition of FR on KB cell surfaces with FA-enriched regular medium and pretreatment with free FA as a competitor prevents FPP from being transported into KB cells (Figure 6d). However, FPP still entered KB cells via nonspecific endocytosis<sup>33</sup> as well as receptor-mediated endocytosis, suggesting the transduction efficiency of FPP is higher even in FR-negative A549 cells (Figure 6c) and the inhibition of transduction was incomplete in the competition assay. HEK 293 and LoVo cells, which showed the highest transfection efficiency of 24–40%, are derived from tumor cells with higher FR expression (Figure 6e).<sup>34</sup> These results are consistent with a previous report showing that targeting efficacy is much poorer in mice on an FA-enriched diet or when excess free FA was preadministered as a receptor blocking agent.<sup>35</sup> The same reason may also explain the discrepancy in transfection efficiency of FPP in the different tumor cell lines.

In contrast to a previous report showing a serum-associated reduction in transfection efficiency,<sup>22</sup> our results suggest that the transfection efficiency of FPP/pDNA is enhanced when conducted in the presence of 10% or 15% FBS (Figure 6b). As the most abundant proteins in serum, FBS can facilitate the transport of vitamins, ions, and drugs in the blood and act as a major pH buffering protein.<sup>36</sup> One possible reason for the enhanced transfection efficiency is that an ionic interaction between cationic FPP/pDNA polyplexes and anionic FBS serves to accelerate the process of endocytosis and reduce the cytotoxicity associated with FPP/pDNA polyplexes. Our results are supported by the studies of Yang et al.<sup>37</sup> and Huang et al.<sup>24</sup> who demonstrated that 2,4-dinitro-1-fluorobenzene-terminated PR derivatives and 2-hydroxypropyl- $\gamma$ -cyclodextrin with an oligopeptide targeting HER2 (HP g-CD-PEI-P) have a high efficiency of gene transfection in medium containing serum in vitro.

To target tumor cells using FPP delivery, the p53 tumor suppressor gene was incorporated into the complex. As a tumor suppressor, p53 inhibits the cell cycle and induces cell apoptosis. The functions of caspases and Bax depend on the p53 gene. In this study, the activities of caspase-9 and bax were significantly enhanced by FPP/DNA (p53) injection in nude mice (Figure 7d), indicating that FPP was able to transfer p53 into tumor cells.

Drug cytotoxicity is mainly observed as damage to liver and spleen cells.<sup>38</sup> No evidence of hepatocellular degeneration or necrosis nor of neutrophil, lymphocyte, or macrophage infiltration was observed. Spleen sinus and liver did not show pathological changes indicating FPP has no cellular toxicity in

vivo. In summary, our results suggest that FPP is a strong candidate to undergo clinical trials for cancer gene therapy.

## ■ ASSOCIATED CONTENT

### ■ Supporting Information

Representative  $^1\text{H}$  NMR spectrum (Figure S1), a panel of five different cell types evaluated for EGFP expression (Figure S2), and the construction of folate-terminated polyrotaxanes (Figure S3). This material is available free of charge via the Internet at <http://pubs.acs.org>.

## ■ AUTHOR INFORMATION

### Corresponding Author

\*Southern Medical University, Department of Pharmaceutical Science, Nanfang Hospital, 1838# Guangzhou Dadaobei Rd., Guangzhou, Guangdong, China, 510515. Tel: 020-61642173 (office or fax). E-mail: [jhchen06@126.com](mailto:jhchen06@126.com).

### Notes

The authors declare no competing financial interest.

## ■ ACKNOWLEDGMENTS

This study was financially supported by the National Science Foundation of China (NSFC) (No. 81173013). We thank Drs. Chao Zhang, Jianye Zhang, Yiwen Tao, Guodong Zheng, and Jun Huang (Department of Pharmaceutical Science, Guangzhou Medical University, Guangzhou) and Lianbing Hou and Guofeng Li (Department of Pharmaceutical Science, Nanfang Hospital, Southern Medical University, Guangzhou) for their kind assistance.

## ■ REFERENCES

- (1) Erbacher, P.; Bettinger, T.; Belguise-Valladier, P.; Zou, S.; Coll, J. L.; Behr, J. P.; Remy, J. S. Transfection and physical properties of various saccharide, poly(ethylene glycol), and antibody-derivatized polyethylenimines (PEI). *J. Gene Med.* **1999**, *1* (3), 210–22.
- (2) Glover, D. J.; Lipps, H. J.; Jans, D. A. Towards safe, non-viral therapeutic gene expression in humans. *Nat. Rev. Genet.* **2005**, *6* (4), 299–310.
- (3) Lopez, A.; Spracklin, D.; McConkey, S.; Hanna, P. Cutaneous mucinosis and mastocytosis in a shar-pei. *Can. Vet. J.* **1999**, *40* (12), 881–3.
- (4) Ogris, M.; Brunner, S.; Schuller, S.; Kircheis, R.; Wagner, E. PEGylated DNA/transferrin-PEI complexes: reduced interaction with blood components, extended circulation in blood and potential for systemic gene delivery. *Gene Ther.* **1999**, *6* (4), 595–605.
- (5) Putnam, D.; Zelikin, A. N.; Izumrudov, V. A.; Langer, R. Polyhistidine-PEG:DNA nanocomposites for gene delivery. *Biomaterials* **2003**, *24* (24), 4425–33.
- (6) Mishra, S.; Heidel, J. D.; Webster, P.; Davis, M. E. Imidazole groups on a linear, cyclodextrin-containing polycation produce enhanced gene delivery via multiple processes. *J. Controlled Release* **2006**, *116* (2), 179–91.
- (7) Koshi, Y.; Nakata, E.; Miyagawa, M.; Tsukiji, S.; Ogawa, T.; Hamachi, I. Target-specific chemical acylation of lectins by ligand-tethered DMAP catalysts. *J. Am. Chem. Soc.* **2008**, *130* (1), 245–51.
- (8) Pereboev, A.; Pereboeva, L.; Curiel, D. T. Phage display of adenovirus type 5 fiber knob as a tool for specific ligand selection and validation. *J. Virol.* **2001**, *75* (15), 7107–13.
- (9) Majumdar, D.; Peng, X. H.; Shin, D. M. The medicinal chemistry of theragnostics, multimodality imaging and applications of nanotechnology in cancer. *Curr. Top. Med. Chem.* **2010**, *10* (12), 1211–26.
- (10) Neu, M.; Fischer, D.; Kissel, T. Recent advances in rational gene transfer vector design based on poly(ethylene imine) and its derivatives. *J. Gene Med.* **2005**, *7* (8), 992–1009.

- (11) Fischer, D.; Li, Y.; Ahlemeyer, B.; Krieglstein, J.; Kissel, T. In vitro cytotoxicity testing of polycations: influence of polymer structure on cell viability and hemolysis. *Biomaterials* **2003**, *24* (7), 1121–31.
- (12) Gong, C. Y.; Wu, Q. J.; Dong, P. W.; Shi, S.; Fu, S. Z.; Guo, G.; Hu, H. Z.; Zhao, X.; Wei, Y. Q.; Qian, Z. Y. Acute toxicity evaluation of biodegradable in situ gel-forming controlled drug delivery system based on thermosensitive PEG-PCL-PEG hydrogel. *J. Biomed. Mater. Res. B, Appl. Biomater.* **2009**, *91* (1), 26–36.
- (13) Li, J.; Loh, X. J. Cyclodextrin-based supramolecular architectures: syntheses, structures, and applications for drug and gene delivery. *Adv. Drug Delivery Rev.* **2008**, *60* (9), 1000–17.
- (14) Cryan, S. A.; Holohan, A.; Donohue, R.; Darcy, R.; O'Driscoll, C. M. Cell transfection with polycationic cyclodextrin vectors. *Eur. J. Pharm. Sci.* **2004**, *21* (5), 625–33.
- (15) Yang, C.; Wang, X.; Li, H.; Goh, S. H.; Li, J. Synthesis and characterization of polyrotaxanes consisting of cationic alpha-cyclodextrins threaded on poly[(ethylene oxide)-ran-(propylene oxide)] as gene carriers. *Biomacromolecules* **2007**, *8* (11), 3365–74.
- (16) Yang, C.; Wang, X.; Li, H.; Tan, E.; Lim, C. T.; Li, J. Cationic polyrotaxanes as gene carriers: physicochemical properties and real-time observation of DNA complexation, and gene transfection in cancer cells. *J. Phys. Chem. B* **2009**, *113* (22), 7903–11.
- (17) Jeong, J. H.; Kim, S. H.; Kim, S. W.; Park, T. G. In vivo tumor targeting of ODN-PEG-folic acid/PEI polyelectrolyte complex micelles. *J. Biomater. Sci., Polym. Ed.* **2005**, *16* (11), 1409–19.
- (18) Lai, C. L.; Lai, L.; Zhao, J. B.; Chen, J. H. Synthesis of polyrotaxane-camptothecin conjugates and evaluation of its anti-tumor effect. *Yao Xue Xue Bao* **2010**, *45* (7), 920–5.
- (19) Chan, P.; Kurisawa, M.; Chung, J. E.; Yang, Y. Y. Synthesis and characterization of chitosan-g-poly(ethylene glycol)-folate as a non-viral carrier for tumor-targeted gene delivery. *Biomaterials* **2007**, *28* (3), 540–9.
- (20) Moon, C.; Kwon, Y. M.; Lee, W. K.; Park, Y. J.; Chang, L. C.; Yang, V. C. A novel polyrotaxane-based intracellular delivery system for camptothecin: in vitro feasibility evaluation. *J. Biomed. Mater. Res. A* **2008**, *84* (1), 238–46.
- (21) Yang, C.; Li, H.; Goh, S. H.; Li, J. Cationic star polymers consisting of alpha-cyclodextrin core and oligoethylenimine arms as nonviral gene delivery vectors. *Biomaterials* **2007**, *28* (21), 3245–54.
- (22) Liang, B.; He, M. L.; Xiao, Z. P.; Li, Y.; Chan, C. Y.; Kung, H. F.; Shuai, X. T.; Peng, Y. Synthesis and characterization of folate-PEG-grafted-hyperbranched-PEI for tumor-targeted gene delivery. *Biochem. Biophys. Res. Commun.* **2008**, *367* (4), 874–80.
- (23) Mansouri, S.; Cuie, Y.; Winnik, F.; Shi, Q.; Lavigne, P.; Benderdour, M.; Beaumont, E.; Fernandes, J. C. Characterization of folate-chitosan-DNA nanoparticles for gene therapy. *Biomaterials* **2006**, *27* (9), 2060–5.
- (24) Yao, H.; Ng, S. S.; Tucker, W. O.; Tsang, Y. K.; Man, K.; Wang, X. M.; Chow, B. K.; Kung, H. F.; Tang, G. P.; Lin, M. C. The gene transfection efficiency of a folate-PEI600-cyclodextrin nanopolymer. *Biomaterials* **2009**, *30* (29), 5793–803.
- (25) Ko, J. K.; Sham, N. F.; Guo, X.; Cho, C. H. Beneficial intervention of experimental colitis by passive cigarette smoking through the modulation of cytokines in rats. *J. Invest. Med.* **2001**, *49* (1), 21–9.
- (26) Kunath, K.; von Harpe, A.; Fischer, D.; Petersen, H.; Bickel, U.; Voigt, K.; Kissel, T. Low-molecular-weight polyethylenimine as a non-viral vector for DNA delivery: comparison of physicochemical properties, transfection efficiency and in vivo distribution with high-molecular-weight polyethylenimine. *J. Controlled Release* **2003**, *89* (1), 113–25.
- (27) Kogel, D.; Fulda, S.; Mittelbronn, M. Therapeutic exploitation of apoptosis and autophagy for glioblastoma. *Anticancer Agents Med. Chem.* **2010**, *10* (6), 438–49.
- (28) He, Z.; Ma, W. Y.; Hashimoto, T.; Bode, A. M.; Yang, C. S.; Dong, Z. Induction of apoptosis by caffeine is mediated by the p53, Bax, and caspase 3 pathways. *Cancer Res.* **2003**, *63* (15), 4396–401.

- (29) Li, J. J.; Zhao, F.; Li, J. Polyrotaxanes for applications in life science and biotechnology. *Appl. Microbiol. Biotechnol.* **2011**, *90* (2), 427–43.
- (30) Lu, B.; Wang, C. F.; Wu, D. Q.; Li, C.; Zhang, X. Z.; Zhuo, R. X. Chitosan based oligoamine polymers: synthesis, characterization, and gene delivery. *J. Controlled Release* **2009**, *137* (1), 54–62.
- (31) Jiang, H. L.; Kim, Y. K.; Arote, R.; Nah, J. W.; Cho, M. H.; Choi, Y. J.; Akaike, T.; Cho, C. S. Chitosan-graft-polyethylenimine as a gene carrier. *J. Controlled Release* **2007**, *117* (2), 273–80.
- (32) Gao, X.; Kim, K. S.; Liu, D. Nonviral gene delivery: what we know and what is next. *AAPS J.* **2007**, *9* (1), E92–104.
- (33) Patri, A. K.; Kukowska-Latallo, J. F.; Baker, J. R., Jr. Targeted drug delivery with dendrimers: comparison of the release kinetics of covalently conjugated drug and non-covalent drug inclusion complex. *Adv. Drug Delivery Rev.* **2005**, *57* (15), 2203–14.
- (34) Cho, K. C.; Kim, S. H.; Jeong, J. H.; Park, T. G. Folate receptor-mediated gene delivery using folate-poly(ethylene glycol)-poly(L-lysine) conjugate. *Macromol. Biosci.* **2005**, *5* (6), 512–9.
- (35) Mathias, C. J.; Wang, S.; Lee, R. J.; Waters, D. J.; Low, P. S.; Green, M. A. Tumor-selective radiopharmaceutical targeting via receptor-mediated endocytosis of gallium-67-deferoxamine-folate. *J. Nucl. Med.* **1996**, *37* (6), 1003–8.
- (36) Quinlan, G. J.; Martin, G. S.; Evans, T. W. Albumin: biochemical properties and therapeutic potential. *Hepatology* **2005**, *41* (6), 1211–9.
- (37) Yang, C.; Li, H.; Wang, X.; Li, J. Cationic supramolecules consisting of oligoethylenimine-grafted alpha-cyclodextrins threaded on poly(ethylene oxide) for gene delivery. *J. Biomed. Mater. Res. A* **2009**, *89* (1), 13–23.
- (38) Ichihara, H.; Funamoto, K.; Matsushita, T.; Matsumoto, Y.; Ueoka, R. Histological bioanalysis for therapeutic effects of hybrid liposomes on the hepatic metastasis of colon carcinoma in vivo. *Int. J. Pharm.* **2010**, *394* (1–2), 174–8.